Temporal Changes in Strain Condition on All Lateral Surfaces during Pretreatment before Timber Drying

Keisuke Toba,[a,]* Takahisa Nakai,[b] and Tomoya Murano [a]

Wood drying, such as boxed-heart square timber, often involves surface checks, which spoils the appearance of wood products and reduces their market value. Pretreatments are performed to avoid the surface checks, but detailed information about surface strain during timber drying remains unclear. In this study, surface strain detections were performed using two types of strain sensors (strain gauge and optical fiber strain sensor) to understand the surface dimensional changes during a series of pretreatments, consisting of steaming and high temperature and low humidity treatment. Simultaneous strain measurements based on the optical fiber sensor grasped the surface strain distributions in each lateral surface during timber drying; contraction behaviors were observed in the middle part of most surfaces in the early steaming stage, while one surface showed expansion. A remarkable expansion was detected in one surface during the high temperature and low humidity treatment, although most of the other surfaces showed gradual contraction behaviors. It was also discovered that the above detected behaviors were gradually reduced with the progress of each pretreatment.

DOI: 10.15376/biores.18.3.4450-4457

Keywords: Wood drying; Surface strain; Japanese cedar; Drying process; Sensing technique

*Contact information: a: Department of Wood Properties and Processing, Forestry and Forest Products Research Institute, Matsunosato, Tsukuba 305-8687 Japan; b: Graduate School of Bioresources, Mie University, Kurimamachiya-cho, Tsu 514-8507 Japan; *Corresponding author: tobak@ffpri.affrc.go.jp*

INTRODUCTION

A living tree usually contains a large amount of moisture; therefore, drying is an inevitable process in using forest resources for wood products in terms of dimensional stability and durability (Shida and Kawasaki 2020). This process often accompanies the occurrence of material defects caused by the loss of moisture in wood cell walls (Kollmann and Côté 1968). Drying also accounts for about half of the volume of greenhouse gas (GHG) emissions in timber production (Fuchigami and Nakai 2020). Thus, optimizing the drying process reduces GHG emissions and the cost of timber production.

In the Japanese wood industry, most structural lumber of softwood species, such as Japanese cedar and hinoki cypress, are often exposed under high-temperature conditions of about 100 °C during kiln drying processes. Especially in drying boxed-heart square timbers, temperatures above 100 °C are commonly adopted immediately after steaming at around 90 °C to suppress surface checks (Yoshida *et al*. 2000, 2004; Kuroda 2007). This is because most consumers in Japan demand a better appearance without surface checks on all lateral surfaces of timber. However, it has also been shown that the excessive duration of the above pretreatment involves the occurrence of internal checks in the latter stage of drying (Yoshida *et al*. 2004; Uehara *et al*. 2005). Thus, many studies have been performed to determine the initial optimal conditions for drying timber (Shida and Kawasaki 2020).

Several studies have investigated temporal changes in the surface strain during drying. For example, Kobayashi and Hisada (1998) used a differential transformer-type sensor to measure the surface strain of flat-sawn timber of *Quercus crispula* based on the temporal changes in the displacement between reference points during drying. They suggested that the drying time can be shortened by controlling the drying schedule based on actual surface strain conditions. Similar studies have also been conducted on the drying of boxed-heart timbers of Japanese cedar (Toba *et al*. 2018; Murano *et al*. 2020). In particular, Murano *et al*. (2020) visualized the two-dimensional in-plane distribution of surface strains based on the image analytical method (Murata 2005), and the obtained results coincided with a numerical simulation (Nakao 2002). However, the above studies detected only one lateral surface due to the measuring equipment. Furthermore, Toba *et al*. (2018) suggested that experimental results occasionally contained symptoms of the surface check of which the expansion cannot be explained by the thermal expansion (Weatherwax and Stamm 1946) and the release of surface growth stresses (Tejada *et al*. 1998; Clair 2012; Toba *et al*. 2013). Considering that it is impossible to entirely predict the occurrence site of surface checks of boxed-heart square timber during drying, further information that enables simultaneous measurement of strain distribution on all lateral surfaces is required to comprehensively understand the surface dimensional changes.

The purpose of this study was to investigate the surface strain condition of boxed-heart square timber during kiln drying. The temporal changes in strain conditions on all lateral surfaces during pretreatment processes were examined using two types of strain sensing techniques.

EXPERIMENTAL

Tested Wood

The studied specimen was prepared using 1000 mm length of a boxed-heart square timber of Japanese cedar (*Cryptomeria japonica* D. Don) from Ibaraki Prefecture, Japan. The pith of the specimen was adjusted to the center of the cross-section during sawing. The size of the cross-section was 100 × 100 mm. Both axial ends of the green specimens were covered with a sealant (SR-066, Cemedine Co., Ltd., Tokyo, Japan). The initial moisture content of the specimen, which was obtained by the oven drying method, was 95.5%. The average width of the annual ring in the specimen was 7.1 mm.

Drying Schedule and Temperature Measurement

The specimen was subjected to a typical drying schedule consisting of successive pretreatments (Kuroda 2007), as shown in Table 1; 6 h of steaming was followed by 21 h of high temperature and low humidity (HTLH) treatment. The former had a temperature of 95 °C for both dry and wet bulbs. The latter was 120 °C for the dry bulb and 90 °C for the wet bulb. The air blow was performed at a velocity of 1 m/s in order to achieve a uniform condition in the dryer during these pretreatments.

After a series of pretreatments, the moisture content of the entire specimen was reduced to 37.3%. If these conditions persist for a long time, the moisture contents will eventually become constant at approximately 22.9% and 2.6% as the equilibrium moisture content, respectively (Saito and Shida 2016). The dry and wet bulb temperatures in a kiln dryer (L-LDA-000, Nihon Denka Kohki Co., Ltd., Tokyo Japan) were measured every minute using a T-type thermocouple (T-2-PEEK-J1, Ninomiya Electric Wire Co., Ltd., Sagamihara, Japan).

Table 1. Drying Schedule of Steaming and High Temperature and Low Humidity (HTLH) Treatment

Pretreatment Type	Time (h)	Dry-bulb Temperature (°C)	Wet-bulb Temperature (°C)
Steaming	6	95	95
HTLH treatment	21	120	90

Surface Strain Measurement

Two types of strain sensors were used to measure the temporal changes in the tangential surface strain of the boxed-heart square timber, as shown in Fig. 1. Three strain gauges (FLA-10-11-2LJQTA, Tokyo Measuring Instruments Laboratory Co., Ltd., Tokyo, Japan) with a gauge length of 10 mm were pasted on all lateral surfaces of the boxed-heart square timber at equal intervals using cyanoacrylate adhesive (CN-E, Tokyo Measuring Instruments Laboratory Co., Ltd., Tokyo, Japan) to detect the changing tangential strains during drying, and the data of strain values were collected every minute using a data logger (TDS-540, Tokyo Measuring Instruments Laboratory Co., Ltd., Tokyo, Japan). The gauge factor related to the measurement accuracy of this strain gauge was 2.10 ± 1%.

Optical fiber strain sensors were also pasted using the same adhesive; threadlike sensors were tangentially fixed in three parts around the boxed-heart square timber (Fig. 1). Surface strains were calculated based on the coordinate information using an optical fiber strain measurement apparatus (FBI-gauge, Fuji Technical Research Inc., Yokohama, Japan). The measurement accuracy of this sensor was 0.2×10^{-3} %. For the first 50 min, strain data were calculated at 1-, 3-, and 5-mm intervals, and then only at 5-mm intervals. All data of strain values were also collected every minute. After attaching the two types of strain sensors, the specimen was placed on two stickers with a cross-section of 3 cm square to ensure the airflow over the entire lateral surfaces of timber during drying.

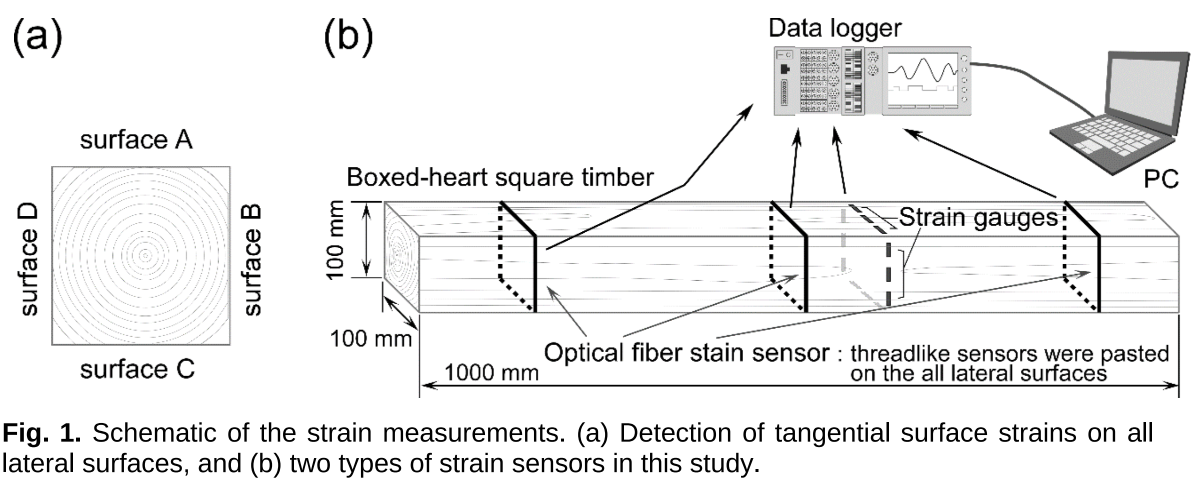

Fig. 1. Schematic of the strain measurements. (a) Detection of tangential surface strains on all lateral surfaces, and (b) two types of strain sensors in this study.

RESULTS AND DISCUSSION

Effects of the Difference in Measurement Method of Surface Strain

Figure 2 shows the typical results of the surface strain distribution obtained by both sensors; all plots in Fig. 2 show the strain values for different parts in the same lateral surface after 50 min of steaming. Strain values estimated by the strain gauge were almost identical to those calculated by the optical fiber sensor at 5 mm intervals (Fig. 2a and b). However, a clearer distribution was detected at 3 mm intervals, as shown in Fig 2c. Although the detected strains did not always fit precisely, it was considered that the concavo–convex shape of the strain distribution in this figure is associated with the surface pattern of annual rings. This idea coincided with some previous studies; the shrinkage of the latewood was considerably higher than the earlywood in the cases of radiate pine and Japanese larch (Nakano *et al*. 2001; Pang and Herritsch 2005). Garcia *et al*. (2022) also verified the difference in shrinking behaviors between earlywood and latewood using the digital image correlation method and indicated the existence of a significant interaction during the swelling of jack pine.

The strain distribution in the lateral surface of drying timber disappeared when the calculation interval was too close, as shown in Fig. 2d. Selecting the optimal resolution for the strain detection clarifies the detailed behaviors of the surface dimensional changes during timber drying.

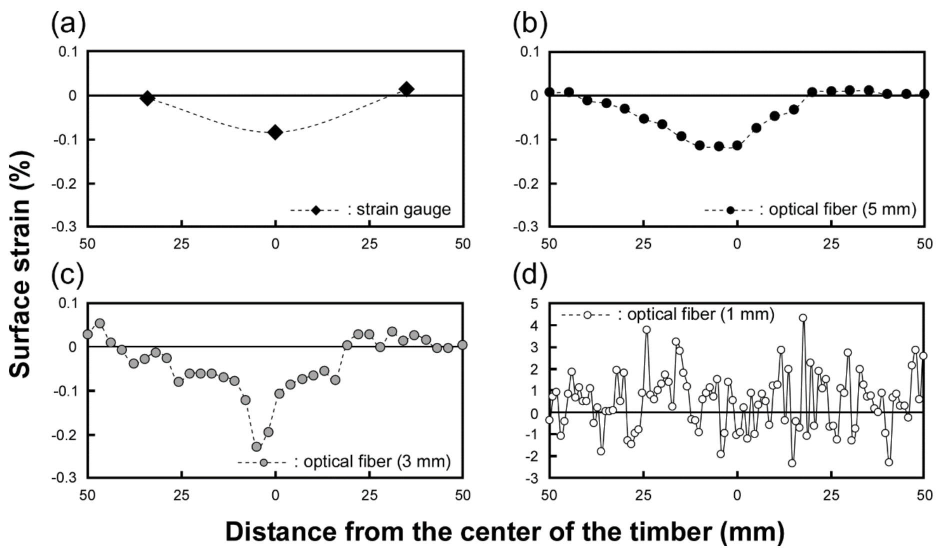

Fig. 2. Tangential surface strains after steaming for 50 min. (a) Detected by strain gauges, (b) optical fiber strain sensor calculated at 5 mm intervals, (c) optical fiber strain sensor calculated at 3 mm intervals, and (d) optical fiber strain sensor calculated at 1 mm intervals

Changes in the Surface Strain during Steaming

Figure 3 shows the temporal changes in tangential strains on all lateral surfaces during steaming. Surface strains showed similar values between the two detection methods. Three of the four surfaces (surfaces A, B, and C) showed contraction behaviors especially in the middle part during the early steaming stages, such as 2 h. These contraction behaviors coincided with previous studies (Toba *et al*. 2018; Murano *et al*. 2020). These initial contraction behaviors gradually decreased, as represented by the comparison between the second and third rows of surface B.

Despite the identical steaming with surface contractions of the timber, only surface D exhibited expansion behavior. This suggested that mechanical interactions due to the other shrinking lateral surfaces offset the contraction behavior of surface D. However, further verifications are required to show the existence of the interactions during timber drying, such as measuring the residual stresses.

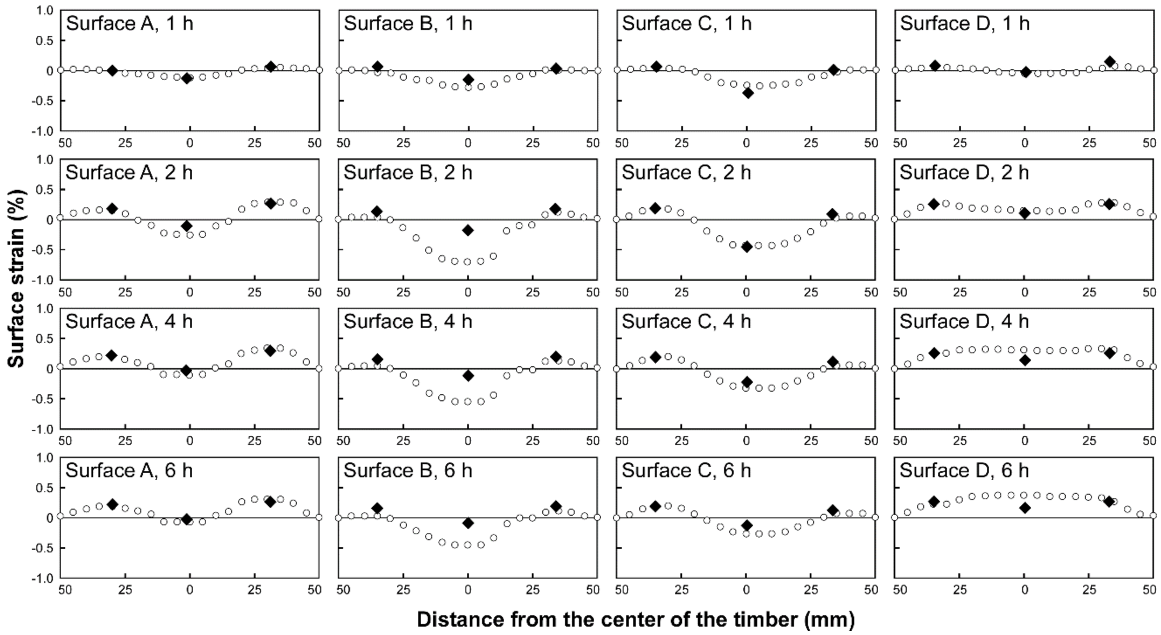

Fig. 3. Temporal changes in tangential strains on all lateral surfaces during steaming. Open circles and filled diamonds indicate the data of surface strain by the optical fiber sensor and strain gauge, respectively. The former was calculated at 5 mm intervals.

Changes in the Surface Strain during High Temperature and Low Humidity Treatment

Figure 4 shows the temporal changes in tangential strains in all lateral surfaces during high temperature and low humidity (HTLH) treatment after steaming. The expansion on all lateral surfaces gradually replaced the above contraction behaviors due to the steaming during the first two hours of this treatment. Remarkable behaviors were observed on surface A; expansion behavior was detected by both strain sensors in the middle part of the surface, as shown in the fourth and fifth rows in the left column in Fig. 4. Similar behavior has also been found and considered to be a symptom of the surface checks in a previous study (Toba *et al*. 2018). This partial expansion was maintained even after 12 h of HTLH treatment and largely disappeared at 21 h, as well as other surfaces. The formation of such strain conditions of timber surfaces brings a better appearance without surface checks in all lateral surfaces, even after the subsequent drying processes. Thus, it is reasonable to avoid an excessive HTLH treatment duration that involves internal checks in the latter stage of drying (Yoshida *et al*. 2004; Uehara *et al*. 2005).

At all events, the simultaneous measurement in all lateral surfaces by the detection technique using an optical fiber sensor made it possible to grasp the distributions of strain conditions in each lateral surface during timber drying. These detailed phenomena are likely to be missed in detection by conventional technique, indicating that a fatal loss can be involved if the drying operation is controlled by the information about strains of only one surface.

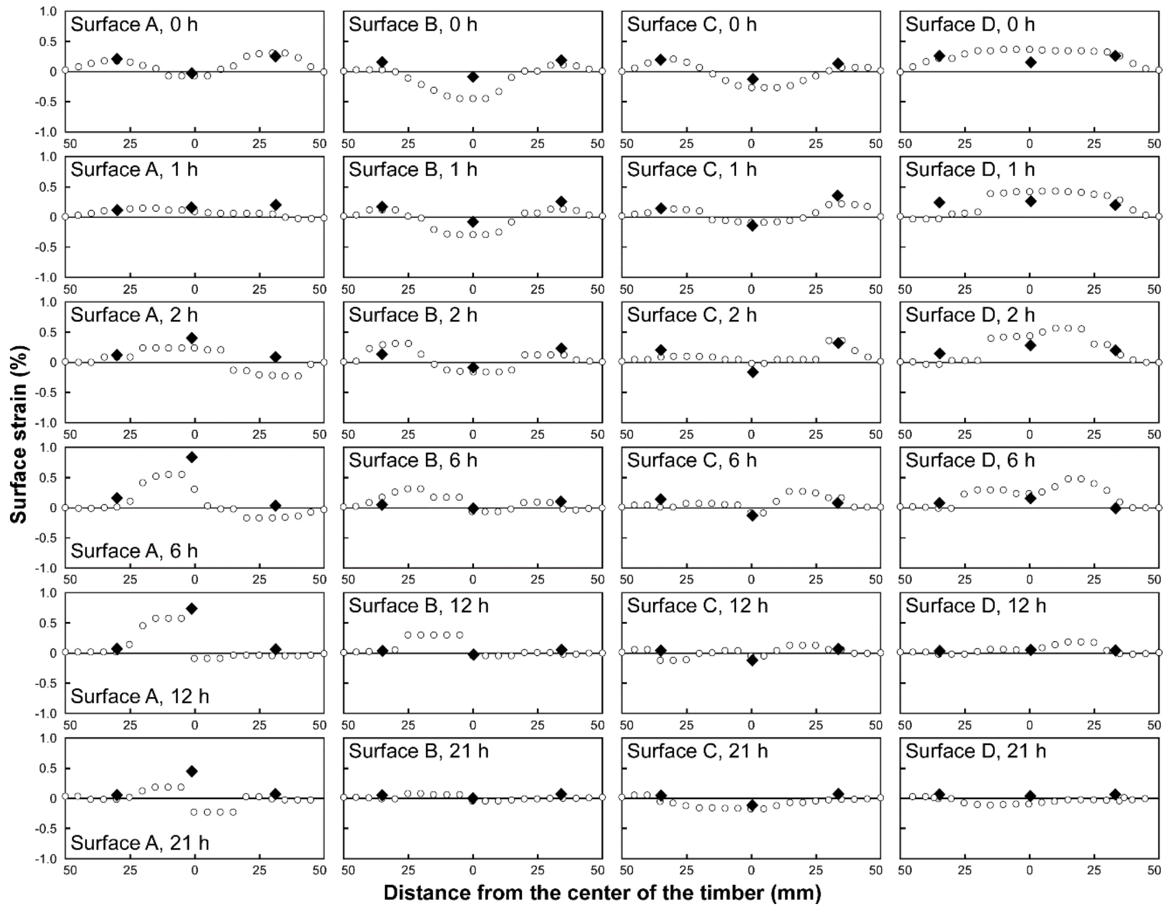

Fig. 4. Temporal changes in tangential strains on all lateral surfaces during HTLH treatment. All symbols here indicate the same as in Fig. 3.

CONCLUSIONS

1. The optimal resolution for the strain detection made it possible to understand the detailed behaviors of the surface dimensional changes during timber drying, such as the partial differences due to the surface tissues of the wood.
2. Contraction behaviors were observed in the middle part of most surfaces in the early steaming stage, while one surface showed expansion. The contractions were gradually reduced during the process of steaming.
3. Remarkable expansion was observed in one surface during the high temperature, low humidity (HTLH) treatment, although most of the other surfaces showed gradual contraction behaviors. This expansion related to the occurrence of surface checks disappearing during HTLH treatment.
4. Simultaneous measurements in all lateral surfaces based on the optical fiber sensor made it possible to understand the detailed distributions of strain conditions in each lateral surface during timber drying.

REFERENCES CITED

Clair, B. (2012). "Evidence that release of internal stress contributes to drying strains of wood," *Holzforschung* 66(3), 349-353. DOI: 10.1515/hf.2011.159

Fuchigami, Y., and Nakai T. (2020). "Evaluation of greenhouse gas emissions associated with lumber products from sawmills in Mie Prefecture, Japan," *Mokuzai Gakkaishi* 66(3), 161-170. DOI: 10.2488/jwrs.66.161

Garcia, R. A., Rosero-Alvarado, J., and Hernández, R. E. (2022). "Moisture-induced strains in earlywood and latewood of mature and juvenile woods in jack pine from 3D-DIC measurements," *Wood Mater. Sci. Eng.* DOI: 10.1080/17480272.2022.2056714

Kobayashi, I., and Hisada, T. (1998). "Application of surface strain measurement to wood drying schedule management," *Wood Industry* 53(2), 69-73.

Kollmann, F. F. P., and Côté, W. A. (1968). *Principles of Wood Science and Technology I*, Springer-1 Verlag, New York. DOI: 10.1007/978-3-642-87928-9

Kuroda, N. (2007). "Development of fundamental research on drying of boxed-heart square timber of sugi (*Cryptomeria japonica*)," *Mokuzai Gakkaishi* 53(5), 243-253. DOI: 10.2488/jwrs.53.243

Murano, T., Fujimoto, N., Nakao, T., Sakagami, H., and Watanabe, K. (2020). "Temporal change in surface-strain distribution of sugi (*Cryptomeria japonica*) square timber during high-temperature drying," *Mokuzai Gakkaishi* 66(3), 140-147. DOI: 10.2488/jwrs.66.140

Murata, K. (2005). "Application of strain distribution analysis using digital image correlation method," *Wood Industry* 60(3), 110-114.

Nakao, T. (2002). "Theoretical analysis of structural lumber drying schedules," *Mokuzai Gakkaishi* 48(4), 241-248.

Nakano, T., Zhu, J., Takeda, T., and Tokumoto, M. (2001). "Shrinkage of wood from planted trees of Japanese larch (*Larix kaempferi* Carriere)," *B. Shinshu Univ. Forests* 37, 23-29.

Pang, S., and Herritsch, A. (2005). "Physical properties of earlywood and latewood of *Pinus radiata* D. Don: Anisotropic shrinkage, equilibrium moisture content and fibre saturation point," *Holzforschung* 59(6), 654-661. DOI: org/10.1515/HF.2005.105

Saito, S., and Shida, S. (2016). "Equilibrium moisture content of wood estimated using the climate data of Japan," *Mokuzai Gakkaishi* 62(5), 182-189. DOI: 10.2488/jwrs.62.182

Shida, S., and Kawasaki, Y (2020). *Wood Science Series 7: Wood Drying I*, Kaiseisha Press, Otsu, Japan.

Tejada, A., Okuyama, T., Yamamoto, H., Yoshida, M., Imai, T., and Itoh, T. (1998). "Studies on the softening point of wood powder as a basis for understanding the release of residual growth stresses in logs," *Forest Prod. J.* 48(7-8), 84-90.

Toba, K., Yamamoto, H., and Yoshida, M. (2013). "Micromechanical detection of growth stress in wood cell wall by wide-angle X-ray diffraction (WAX)," *Holzforschung* 67(3), 315-323. DOI: 10.1515/hf-2012-0080

Toba, K., Kobayashi, I., Yamamoto, H., and Kurita, S. (2018). "Surface shrinking and swelling behavior of boxed-heart timber of sugi (*Cryptomeria japonica*) during drying using high temperature setting treatment," *Wood Industry* 73(12), 550-554.

Uehara, T., Watahiki, M., Nishino, Y., and Sakuno, T. (2005). "Relationships between internal cracks and strains during high temperature drying of sugi boxed-heart square timbers," *Mokuzai Gakkaishi* 51(4), 243-248. DOI: 10.2488/jwrs.51.243

Yoshida, T., Hashizume, T., and Fujimoto, N. (2000). "High-temperature drying characteristics on boxed-heart square timber of karamatsu and sugi: Influences of high temperature conditions with low humidity on drying properties," *Wood Industry* 55(8), 357-362.

Yoshida, T., Hashizume, T., Takeda, T., Tokumoto, M., and Inde, A. (2004). "Reduction of surface checks by the high-temperature setting method on kiln drying of sugi boxed-heart timber without back-splitting," *J. Soc. Mater. Jpn*. 53(4), 364-369. DOI: 10.2472/jsms.53.364

Weatherwax, R.C., and Stamm, A. J. (1946). *The Coefficients of Thermal Expansion of Wood and Wood Products*, U.S. Department of Agriculture, Forest Products Lab, Madison, WI, USA.

Article submitted: March 29, 2023; Peer review completed: April 15, 2023; Revised version received and accepted: April 28, 2023; Published: May 4, 2023.
DOI: 10.15376/biores.18.3.4450-4457